

EERA DeepWind'2014, 11th Deep Sea Offshore Wind R&D Conference

First verification test and wake measurement results using a Ship-LIDAR System

G. Wolken-Möhlmann*, J. Gottschall, B. Lange

Fraunhofer IWES, Am Seedeich 45, 27572 Bremerhaven, Germany

Abstract

Measuring wind offshore in deep water depths will be a future challenge. Where the sea bed foundation installation for fixed meteorological masts is impossible, floating systems tend to be a sophisticated solution. In addition to the use of moored lidar-buoy systems, ship-lidar systems are an alternative solution for a number of different applications. In this paper we describe general aspects of motion influences on lidar measurements as well as two motion-correction methods for motion-influenced lidar measurements. The implementation of the ship-lidar system and different scanning modes will be presented. First measurements were carried out as part of the EERA-DTOC project. Hence a verification of one of the two correction algorithms as well as first results from wake measurements behind the Alpha Ventus offshore wind farm will be shown. This comprises distinct wind speed wake losses and an increasing turbulence intensity in a distance of approximately 2 km behind the wind farm.

© 2014 Elsevier Ltd. This is an open access article under the CC BY-NC-ND license

(<http://creativecommons.org/licenses/by-nc-nd/3.0/>).

Selection and peer-review under responsibility of SINTEF Energi AS

Keywords: Measurements; lidar; ship-based; offshore; wake; floating lidar;

1. Introduction

The number of lidar-buoy projects has increased dramatically during the last years. The combination of higher flexibility and lower costs compared to ground-fixed meteorological (met.) masts is attractive, and there are joint efforts in order to approve the obtained data as bankable [6]. Still there are a number of scenarios where the flexibility of buoy-based systems does not match the needs, e.g. if the location has to be changed often, or if a vessel in proximity to the location of interest is available, that can be used as a platform for the measurement device.

A first ship-based measurement performed by Fraunhofer IWES was described in [4]. For the operation of lidar systems on ships, motion correction algorithms for floating lidar have to be adapted and implemented for ship measurements, compare [7]. Simplifications are applied under the assumption of neglectable effects of tilting for a faster and simpler processing of the data.

The experimental set-up described here combines a standard lidar system, motion sensors, a computer and wireless router in a frame. The complete ship-lidar system was installed on an offshore support vessel for two measurement

* Corresponding author. Tel.: +49-471-14290-353 ; fax: +49-471-14290-111.

E-mail address: gerit.wolken-moehlmann@iwes.fraunhofer.de

campaigns performed in August and October 2013 as part of the EERA-DTOC project with the aim of measuring wake effects. Results from the measurements with a focus on far-wake detection will be presented.

2. Motion influences on lidar measurements

Wind lidar detect the Doppler shift of the wind velocity v_{LoS} in the line of sight (LoS), defined by

$$\vec{\sigma} \cdot \vec{u} = o_x \cdot u_x + o_y \cdot u_y + o_z \cdot u_z = v_{LoS} \quad (1)$$

where $\vec{\sigma}$ defines the orientation of the laser beam/LoS and \vec{u} is the wind velocity in the measurement volume. If the laser beam is pointed in a number of different directions $\vec{\sigma}_{1..n}$, we interpret the measurement data as a linear system of equations (LSE):

$$\begin{bmatrix} o_x(t_1) & o_y(t_1) & o_z(t_1) \\ o_x(t_2) & o_y(t_2) & o_z(t_2) \\ \vdots & \vdots & \vdots \\ o_x(t_n) & o_y(t_n) & o_z(t_n) \end{bmatrix} \cdot \begin{bmatrix} u_x(\vec{x}_1, t_1) & u_x(\vec{x}_2, t_2) & \cdots & u_x(\vec{x}_n, t_n) \\ u_y(\vec{x}_1, t_1) & u_y(\vec{x}_2, t_2) & \cdots & u_y(\vec{x}_n, t_n) \\ u_z(\vec{x}_1, t_1) & u_z(\vec{x}_2, t_2) & \cdots & u_z(\vec{x}_n, t_n) \end{bmatrix} = \begin{bmatrix} v(\vec{x}_1, t_1) \\ v(\vec{x}_2, t_2) \\ \vdots \\ v(\vec{x}_n, t_n) \end{bmatrix} \quad (2)$$

Under the assumption of spatial and temporal homogeneity for the wind field on each height layer, the LSE is reduced to

$$\begin{bmatrix} o_x(t_1) & o_y(t_1) & o_z(t_1) \\ o_x(t_2) & o_y(t_2) & o_z(t_2) \\ \vdots & \vdots & \vdots \\ o_x(t_n) & o_y(t_n) & o_z(t_n) \end{bmatrix} \cdot \begin{pmatrix} u_x(h) \\ u_y(h) \\ u_z(h) \end{pmatrix} = \begin{bmatrix} v(h, t_1) \\ v(h, t_2) \\ \vdots \\ v(h, t_n) \end{bmatrix} \quad (3)$$

$$\Rightarrow O_{t_1:t_n} \cdot \vec{u} = \vec{v}_{LoS} \quad (4)$$

Here the matrix $O_{t_1:t_n}$ contains the beam orientations for the measurements for different points in time, whereas the vector \vec{u} represents the wind velocity which is defined by the solution of the LSE. \vec{v}_{LoS} contains the obtained wind speeds in LoS and represents only a vector in a mathematical sense. For solving this LSE, at least three linear independent LoS-orientations are necessary. Having more than three different orientations, a least-squares approach has to be applied for solving the LSE.

2.1. Motion effects on lidar measurements

Effects of different kinds of motions as well as the effect of correction algorithms on wind lidar measurement were studied in [2] by using simulations. Similar results were described in [5]. A deeper analysis of the dependence of the inflow wind direction and the motion were studied in [3], with a comparison between simulation and experimental data. Due to rotational motions, the lidar system as well as the beam orientations are tilted. These changes in the orientation of the laser beams are considered within the LSE by using the tilted orientation matrix O_{tilt} .

For measurement under translatory motions, the systems obtains a velocity composed of the wind velocity and system velocity projected on the line of sight:

$$v_{LoS}^{wind} = v_{LoS}^{obtained} - v_{LoS}^{system} \quad (5)$$

For calculating the system velocity in line of sight v_{LoS}^{system} , the line of site and the system velocity must be defined in the same coordinate system, like the system-fixed coordinate system or the local fixed coordinate system.

Considering system velocity and rotations, the LSE for floating lidar is described by

$$O_{tilt} \cdot \vec{u} = v_{LoS}^{obtained} - v_{LoS}^{system} \quad (6)$$

where O_{tilt} and v_{LoS}^{system} are data from the motion sensor and lidar configuration, and $v_{LoS}^{obtained}$ is the information acquired by the lidar measurement. The solution of this LSE combined with a height interpolation describes the complete motion correction.

2.2. Motion time scales and simplified motion correction

Rotational and translatory motions can affect lidar measurements in quite different ways, depending on the time scale of the motion. The reference time scale is the time period needed for a complete lidar measurement, which is the time covered by the LSE. For commercial wind lidar systems, this is the period for obtaining a whole velocity-azimuth display (VAD) scan. Time scale for a Leosphere WindCube V2 comprises 3.5 seconds, whereas the ZephIR lidar performs a whole VAD-scan in one second.

If the time scales of motion and orientation changes are much longer than the reference time scale, O_{tilt} and v_{LoS}^{system} can be assumed as constant. As a result, the motion influences are constant for the whole LSE, and the correction can be applied after calculating the solution of the LSE for fixed systems, the wind vector \vec{u} . Here, we get

$$\vec{u}_{wind}(t) = R_{yaw,pitch,roll,t} \cdot \vec{u}_{measured}(t) - \vec{u}_{system}(t) \quad (7)$$

where $\vec{u}_{measured}(t)$ is the solution of the LSE, $R_{yaw,pitch,roll,t}$ the rotation matrix for one point in time and $\vec{u}_{system}(t)$ the ship velocity vector. Furthermore the equation can be simplified under the assumption of a quite stable platform without dynamic tilting and static tilting angle offsets to

$$\vec{u}_{wind}(t) = R_{yaw,t} \cdot \vec{u}_{measured}(t) - \vec{u}_{system}(t) \quad (8)$$

This correction method, referred to as simplified correction, gives the opportunity for a faster implementation of motion correction as well as a first check of lidar and motion data before applying the complete motion correction. Nevertheless it has to be checked if the assumptions are fulfilled.

3. Measurements

As part of the EERA-DTOC project, two measurement campaigns were performed. The measurements were planned for the determination of wind turbine and wind farm wakes in different downwind distances. In this section, the measurement set-up, the campaigns and the scanning patterns for wake measurements are described.

3.1. Ship-lidar measurement set-up

The ship-lidar system used for the wake measurements comprises a lidar, motion sensors, communication devices and a ruggedized computer. The main component is a Leosphere Windcube V2 Offshore edition. The lidar performs a velocity-azimuth display (VAD) scanning pattern including a fifth vertical beam. A combination of a xSens MTi-G attitude and heading reference sensor (AHRS) and a Trimble SPS361 satellite compass is used for obtaining motion information needed for the correction of the lidar data. The MTi-G sensor has a static accuracy better than 0.5° and is used with a sampling frequency of approx. 10 Hz. The satellite compass has a heading precision of under 0.1° for the here used configuration.

GPS time is used for all sensors to ensure a synchronized data acquisition. The data from the AHRS and compass are logged by the computer. For the current version of the system, lidar data are stored automatically on the lidar system, and are only synchronized manually with the computer. The system can be assessed using wireless connection. This allows to check and control the operation of the lidar and the sensors continuously without direct ethernet access, which is important for measurements under harsh offshore conditions, especially extreme roll angles.

Sensors, computer and communication devices are installed in a waterproof box. The ship-lidar measurement system consists of three separate parts (lidar, sensor box and frame) which are transported onto the ship separately and assembled on board. The frame defines the geometry between the sensors and the lidar, which is important for the correction of the data (see figure 1, left).

For the EERA-DTOC wake measurement campaigns, the ship-lidar was installed on the top deck of the offshore support vessel LEV Taifun, see figure 1, right. The LEV Taifun has an overall length of 41.45 m and a displacement of 330 t. The cruising speed is approximately 8 kn (4 m/s), for the wake measurements the speed was reduced to 2-4 kn (1-2 m/s). The altitude of the top deck was 7 m over sea level, the roll period was approx. 5 s with maximum roll angles up to 20° .

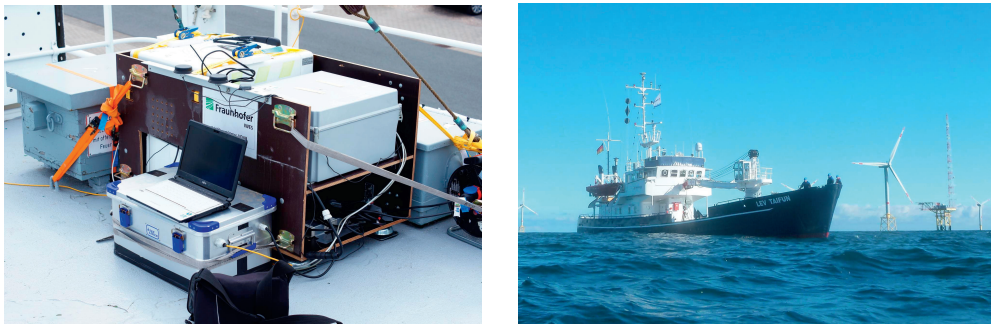


Fig. 1. (a) Lidar and sensor box installed in the frame, fixed to the top deck of the LEV Taifun; (b) LEV Taifun during second measurement campaign in proximity to FINO1.

3.2. Ship-lidar scanning modes

For the detection of wakes using ship-based lidar, three different scenarios for ship tracks, here called scanning modes, are possible:

1. Fixed position in the wake,
2. translational motion along the center of the wake and
3. translational motions perpendicular to the wake,

compare figure 2.

The first mode can be used for smaller wind turbines under very controlled conditions and for smaller distances. The possibility of turning the wind turbine on and off gives the opportunity for obtaining the reference wind conditions and smaller sizes of the wind turbine as well as shorter distances to the turbine decrease the spatial position adjustment due to inflow wind direction changes, see [1]. Nevertheless also small changes in the inflow wind change the location in the wake, whose exact position is difficult to detect.

The second method gives the possibility of detecting the development of the wake with the distance. Assuming a rotor diameter of $D = 120$ m, a scan distance from $10D$ to $70D$ and a mean ship speed from 2 m/s, the resulting measurement period covers approximately one hour. Changes in wind direction of 5° lead to displacement of the wake center of approximately 8.7% of the distance to the turbine, which makes it hard to keep the position in the center of the wake for the whole measurement period.

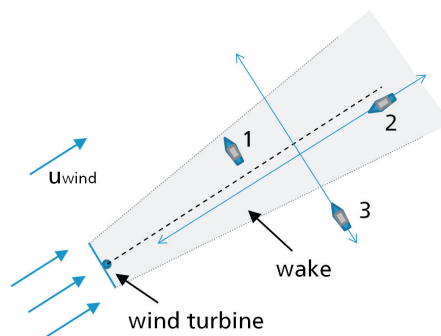


Fig. 2. Different motion patterns for ship-lidar wake measurements: (1) fixed position in the wake, (2) translational motion along the wake center, (3) translational motions perpendicular to the wake.

The third method makes slices in different downwind distances through single wind turbine wakes and the wind farm wake, respectively. Typical time scales for passing a typical wake diameter of approximately $D_{wake} = 200$ m, the turbine distances of 800 m and a wind farm width of 2400 m as well as a mean ship speed of 2 m/s, can be estimated as 100 s for a single wake, 400 s for the passing from one single wake to another single wake and 20 minutes passing a complete wind farm wake. Hence it is expected, that at least for the period of passing a wake the wind conditions are more or less constant. Another advantage of this scanning mode is, that wind speed measurements outside of a wind turbine wake can be used as inflow reference wind speed.

The ship course for the wake measurements is calculated using an algorithm with input parameters of wind direction and defined distances to the center of the Alpha Ventus wind farm. Due to possible changes in inflow wind direction, the ship course has to be checked and adjusted regularly.

For the here used VAD-scan, the different measurement volumes are spatially separated in the magnitude of the obtained altitude level. This means, that single small-scale turbulence occurrences cannot be detected by this kind of scanning pattern. As a consequence, the ship-lidar system is only used for far-wake measurements with a distance of at least 2 km in order to detect a developed and broader wake wind profile. Furthermore the geometry of the offshore wind farm and the inflow wind conditions affect the kind of wake that is generated by superposition of a number of single wakes. Single wakes can only be detected from turbines located at the corner of the wind farm by special inflow wind directions. Measurements within the farm are difficult due to allowances; furthermore, the wakes and small scale turbulence distort the measurement method.

3.3. Measurement campaigns

Two measurement campaigns in the Alpha Ventus wind farm were performed, the first from 27-31 August 2013, and the second from 4-10 October 2013. Due to the transit time from Bremerhaven, Germany, to the Alpha Ventus offshore wind farm of approximately ten hours, the first and last days of each measurement period could not be used for measurements, leaving all together eight days for experiments.

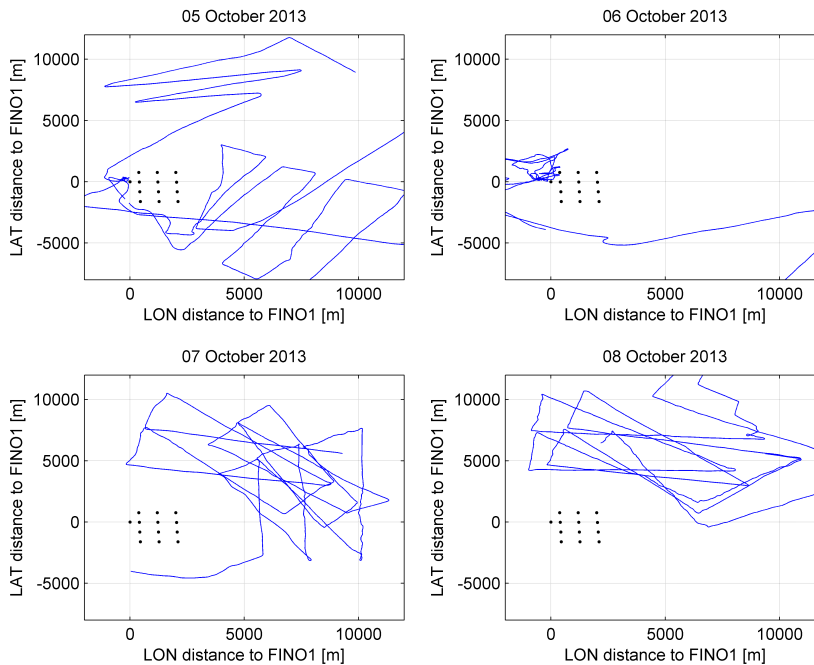


Fig. 3. The daywise ship tracks of the second measurement campaign.

The focus of the first measurement was on system testing, system verification and first near-wake test measurements. For the system verifications, different motion modes, like anchored, translatory motions in and perpendicular to the inflow direction as well as frequent turns in proximity to the meteorological (met.) mast FINO1 were performed. First wake measurements in distances between 1.3 km and 3.5 km downwind distance were executed. Reference wind speeds from the 100 m top anemometer of FINO1 varied between 1.3 m/s and 10.6 m/s with an average of 6.2 m/s, with predominant wind directions from West.

During the second campaign, a number of wake measurements under different distances to Alpha Ventus wind farm were performed. Here the second day of measurement was used for a second verification measurement in proximity to FINO1. The wind velocity for the FINO1 top anemometer varied from 3.0 m/s to 16.1 m/s with a mean value of 7.6 m/s. Wind directions varied from 180° to 320° , with main wind direction from South-West.

Figure 3 shows the ship tracks for four days of the second measurement campaign. The adjusted ship tracks dependent on the varying wind directions can be clearly seen. Due to roll resonance effects under tracks perpendicular to the inflow wind and thus the wind induced waves, the real tracks often had to be yawed slightly compared to the calculated ones.

4. Results

Main goal of the measurement were the wind measurements in the wind turbine wake. Due to the fact that ship based lidar measurements are quite new, a preliminary test was performed as a verification of the measurement principle and motion correction in proximity to FINO1. Furthermore, first results from detected wakes will be presented.

4.1. Comparison between measured and corrected data

In a first part of the data post processing and analysis, the data were corrected using the simplified correction algorithm. In a first step, the wind vector obtained by the lidar was turned corresponding to the yaw measured by

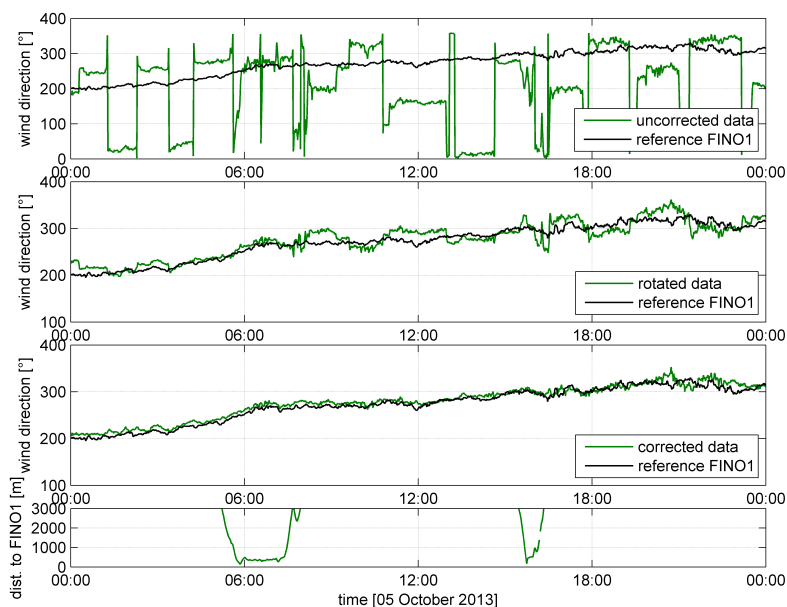


Fig. 4. Comparison between 1-minute-mean wind direction data from FINO1 and ship-lidar for different levels of correction: uncorrected, rotated, rotated and ship velocity.

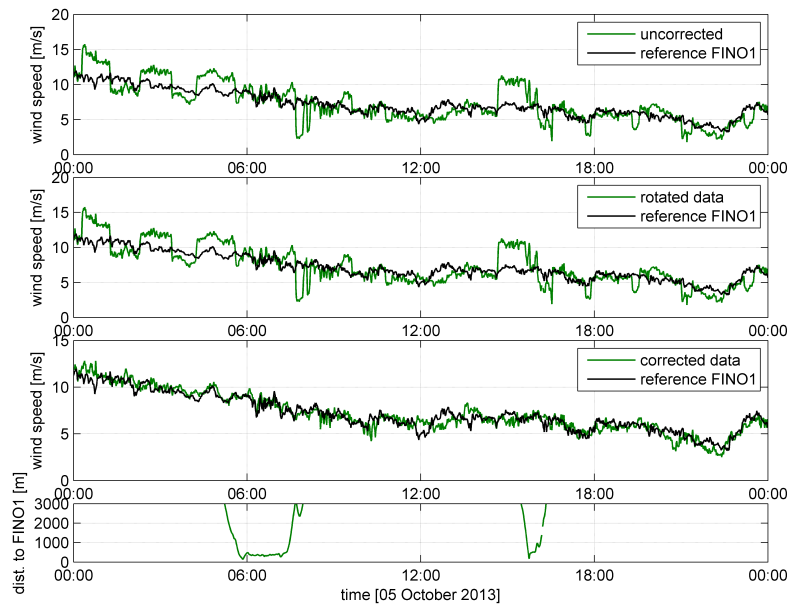


Fig. 5. Comparison between 1-minute-mean wind speed data from FINO1 and ship-lidar for different levels of correction: uncorrected, rotated, rotated and ship velocity.

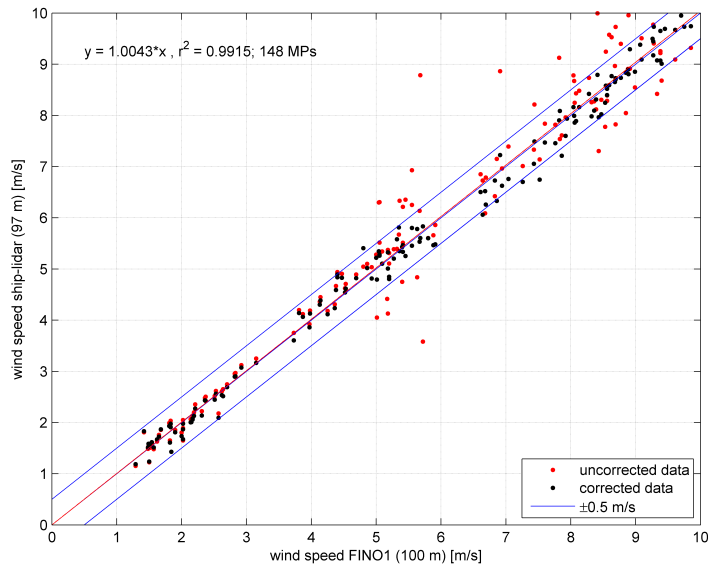


Fig. 6. Wind speed scatter plot between FINO1 and ship-lidar data for 10-min-mean values. Uncorrected (red) as well as corrected data (black) are shown.

the compass. Then, the ship velocity was subtracted from the rotated wind vector. Figure 4 shows the results for the wind direction. Here the ship turning has the predominant influence on the measured wind direction, nevertheless

considering the ship velocity has some effect on improving the data. On the other hand, rotation does not affect the wind speed, as expected. Considering translatory motions improves the wind speed data, see figure 5. Beside the wind direction and wind speed time series, the distance to FINO1 is plotted in order to indicate periods in proximity to the met. mast.

4.2. Direct comparison between ship-lidar and FINO1

In Addition to a qualitative comparison of wind speed and directional data, the measured and corrected wind speed for 10-minutes mean values were plotted versus reference data from FINO1, see figure 6. Measurement points were filtered for met. mast influenced wind directions and to high distances between the ship and FINO1. After applying the correction algorithm, most measurement points are located in an interval of ± 0.5 m/s around the linear regression fit with a slope of 1.0043. With a coefficient of determination of $r^2 = 0.9915$, the corrected data lies within the acceptance criteria for best practice defined by [8], but the values are still low compared to current lidar-buoy measurements, compare [6].

It is assumed that reasons for this is the simplified correction algorithm. Especially extreme ship roll motion with amplitudes of up to 20° and periods of $t \approx 5$ s are not negligible, and furthermore are close to the measurement period of 3.5 s for a WindCube VAD-scan. As a consequence, beating-frequency effects can occur and also influence averaged data. This, as well as the effects of the implementation of the complete motion correction, will be studied more intensely in future work.

4.3. Wake measurements

The ship-lidar wake measurements were performed at various distances to the Alpha Ventus wind farm. In order to detect time periods with a ship position in proximity to the wind turbine wakes, the distance to the wake center was calculated using FINO1 wind direction data and the ship position as input parameters. Due to the duration of the ship inside the wake of approximately two minutes, floating averages comprising a time period of 60 seconds in ten second steps are calculated. Therefore, obtained turbulence intensities cannot be compared to standard 10-min-mean values. Also the turbulence intensity is heavily influenced by the roll motion, which is not considered in the simplified correction method.

One issue of detecting wakes is the discrimination of wake wind speed deficits and wind speed changes caused by inflow turbulence. Therefore a reference wind speed measurement is important. Here FINO1 measurement data are limited as reference, due to the nature of these data coming from point measurements. Furthermore, the distance from the met. mast to the ship, resulting in time shifts of the obtained wind data because of the time of flight of approximately a couple of minutes from mast to the ship lidar, is problematic.

An overview of the data for one cut through the wakes for a downwind distance of approximately 2 km is shown in figure 7. Here the course of the ship, the position of the wind farm as well as the estimated wakes are plotted on the left, where the corrected wind speed and turbulence data can be studied on the right. Due to the inflow wind direction from West, the lidar detects an interference of three wakes for each wind farm row. In the plots, these triple wake can be detected by a distinct decrease in wind speed and an increase of turbulence intensity. The wind velocity deficits were detected in a temporal distance of eight minutes, which refers to approx. 900 m and corresponds to the distance of the Alpha Ventus wind turbines.

For a more detailed analysis, wind speeds and turbulence intensities are plotted for four chosen altitudes, 50 m, 80 m, 110 m and 150 m, see figure 8. From undisturbed reference wind speeds of approximately 6.3 m/s before and 6.8 m/s after the wake measurements, the wind speed drops to 4.5 m/s in the wake center. In between these triple wakes, the wind speed nearly recovers to the reference wind speed. This shows that under westerly winds the wind turbine wakes do not combine to a wind farm wake for a distance of 2 km, which refers to 17 wind turbine rotor diameter. Furthermore, the 1-min-mean turbulence intensity is clearly increasing from approx. 8% to up to 18%. Here it must be mentioned, that the turbulence intensity is influenced by the roll motion which is not considered yet in the data correction.

For wake measurements under longer distances to the wind farm, the analysis of the data is more complicated due to the development of the wakes and the recovery of the wind speed. Here the wake could be detected by an increased

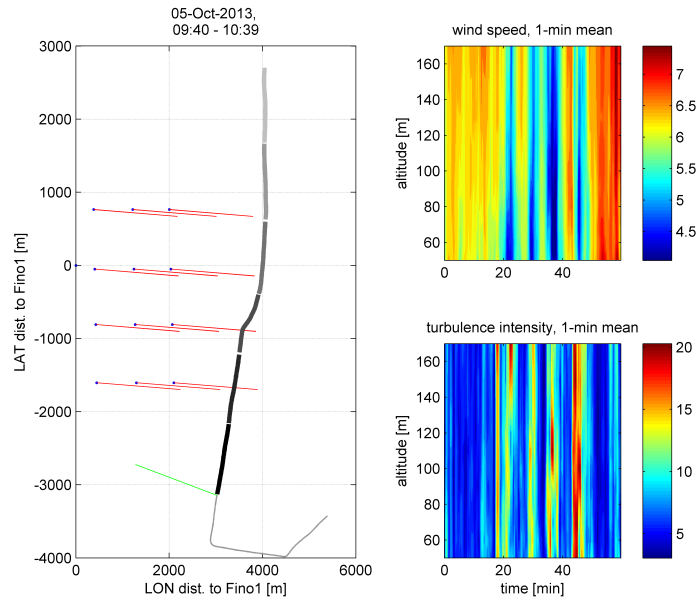


Fig. 7. Comparison of ship track (grey), Alpha Ventus wakes calculated from measured wind direction (red), and the measured wind speed and turbulence intensity (upper right). Furthermore, course over ground and roll angle standard deviation are plotted.

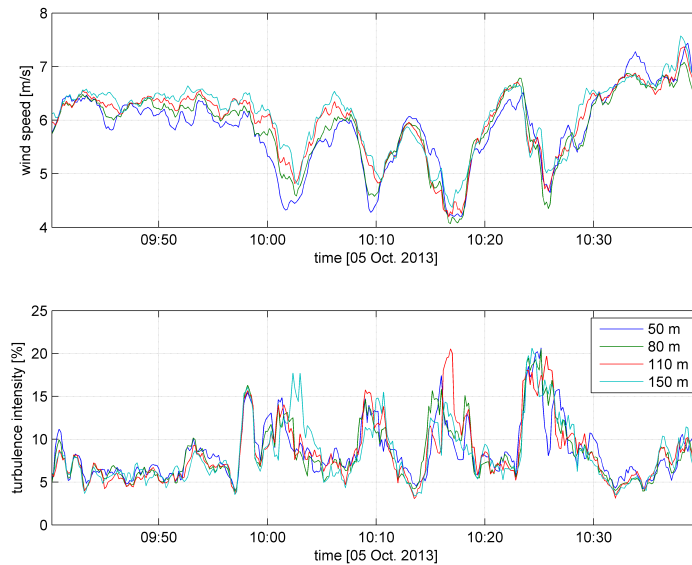


Fig. 8. Example for a wake measurement with a downwind distance of approximately 2 km. The upper plot shows the wind speed and the lower plot the 1-min-mean turbulence intensity. Values are given for the altitudes 50 m, 80 m, 110 m and 140 m. The turbulence intensity is partly influenced by roll motions.

turbulence intensity, which demands for the application of the complete motion correction. Furthermore different inflow wind directions change the superposition of the single wakes and thus the wind farm wake characteristic.

5. Conclusions

First ship-based lidar wake measurements were presented. As a preliminary verification of the system, a comparison between FINO1 reference data and the corrected data was performed. The results show distinct improvements compared to uncorrected data, but the quality of the measured data does not reach the quality of lidar buoy data. A reason for this is supposed to be the simplified correction algorithm which does not consider tilt motions. These motions influence the measured turbulence intensity as well as averaged values due to beating frequency effects between the lidar and the motion. Nevertheless it is assumed that the implementation of the complete motion correction as a next step will improve the data significantly.

During the wake measurements, wind velocity deficits as well as an increasing of the turbulence is clearly visible for distances up to two km from the next turbines. For longer distances, using the simplified motion correction, results are not clear yet. Therefore the complete motion correction is necessary to distinguish between wake induced measured turbulence intensity and motion induced turbulence.

References

- [1] Barthelmie RJ, Folkerts L, Ormel FT, Sanderhoff P. Offshore wind turbine wake measured by sodar. *J. Atmos. Oceanic Technol.*, 20, 466-477, 2003
- [2] Wolken-Möhlmann G, Lilov H, Lange B. Simulation of motion induced measurement errors for wind measurements using LIDAR on floating platforms. *Proceedings 15th International Symposium for the Advancement of Boundary-Layer Remote Sensing (ISARS)*, Paris, France, 28-30 June 2010
- [3] Gottschall J, Wolken-Möhlmann G, Lange B. About offshore resource assessment with floating lidars with special respect to extreme wind structures, *The Science of Making Torque from Wind*, Oldenburg, Germany, 2012
- [4] Wolken-Möhlmann G, Gottschall J, Lilov H, Schillo B, Viergutz Th, Lange B. Ship based lidar measurements, *Proceedings DEWEK*, Bremen, Germany, 2012
- [5] Schlipf D, Rettenmeier A, Haizmann F, Hofsäß M, Courtney M, Chenk PW. Model based wind vector field reconstruction from lidar data. *Proceedings DEWEK*, Bremen, Germany, 2012
- [6] Flower P. Paths towards bankability of floating lidar data, *DNV-GL, Presentation EWEA Offshore*, Frankfurt, Germany, 2013
- [7] Sparling LC, Rabenhorst S, William B, Delgado R, Strobach E, Boicourt B, Bailey B. Building a Science-Based Foundation for Assessing the Offshore Wind Resource of Maryland, *Proceeding EWEA Offshore*, Frankfurt, Germany, 2013
- [8] Carbon Trust Offshore Wind Accelerator roadmap for the commercial acceptance of floating LIDAR technology, Carbon Trust, CTC819 Version 1.0, 21 November 2013